[CANCER RESEARCH 61, 8624–8628, December 15, 2001]

Advances in Brief

Gastrointestinal Stromal Tumors with *KIT* Mutations Exhibit a Remarkably Homogeneous Gene Expression Profile[1]

Susanne V. Allander, Nina N. Nupponen, Markus Ringnér, Galen Hostetter, Greg W. Maher, Natalie Goldberger, Yidong Chen, John Carpten, Abdel G. Elkahloun, and Paul S. Meltzer[2]

Cancer Genetics Branch, National Human Genome Research Institute, NIH, Bethesda, Maryland 20892

Abstract

Gastrointestinal stromal tumors (GISTs), the most common mesenchymal tumors of the digestive tract, are believed to arise from the interstitial cells of Cajal. GISTs are characterized by mutations in the proto-oncogene *KIT* that lead to constitutive activation of its tyrosine kinase activity. The tyrosine kinase inhibitor STI571, active against the BCR-ABL fusion protein in chronic myeloid leukemia, was recently shown to be highly effective in GISTs. We used 13,826-element cDNA microarrays to define the expression patterns of 13 *KIT* mutation-positive GISTs and compared them with the expression profiles of a group of spindle cell tumors from locations outside the gastrointestinal tract. Our results showed a remarkably distinct and uniform expression profile for all of the GISTs. In particular, hierarchical clustering of a subset of 113 cDNAs placed all of the GIST samples into one branch, with a Pearson correlation >0.91. This homogeneity suggests that the molecular pathogenesis of a GIST results from expansion of a clone that has acquired an activating mutation in *KIT* without the extreme genetic instability found in the common epithelial cancers. The results provide insight into the histogenesis of GIST and the clinical behavior of this therapeutically responsive tumor.

Introduction

GISTs[3] are the most common mesenchymal tumors of the digestive tract and are characterized by expression of KIT (stem cell factor receptor, or CD117; for reviews see Refs. 1, 2). The clinical spectrum varies from benign solitary tumors to abdominal spread with multiple tumors and liver metastases. GISTs have been suggested to originate from the ICC or from a stem cell differentiating toward an ICC phenotype (3). ICCs form a cellular network with pacemaker activity in the gut, and KIT expression is essential for the normal development of this network (2). CD34, a marker expressed in ~70% of GISTs, can also be found in mesenchymal cells within the gut wall (1, 2). A large proportion of GISTs are characterized by mutations in the *KIT* gene, predominantly in exon 11, which cause ligand-independent activation of its tyrosine kinase function and capacity to induce malignant transformation *in vitro* (1, 4). Remarkably, the tyrosine kinase inhibitor STI571, which is active against the BCR-ABL fusion protein in CML, was recently shown to be highly effective in GISTs (5–7). To better understand the molecular basis of GIST tumorigenesis, we determined the gene expression profile of GIST, using 13,826-element cDNA microarrays.

Received 8/13/01; accepted 10/30/01.

The costs of publication of this article were defrayed in part by the payment of page charges. This article must therefore be hereby marked *advertisement* in accordance with 18 U.S.C. Section 1734 solely to indicate this fact.

[1] S. V. A. was partly supported by a fellowship grant from the Swedish Medical Research Council, M. R. was supported by a postdoctoral fellowship from the Swedish Research Council, and N. N. was supported in part by the Finnish Cultural Foundation.

[2] To whom requests for reprints should be addressed, at National Human Genome Research Institute, NIH, 49 Convent Drive, Bethesda, MD 20892. Phone: (301) 594-5283; Fax: (301) 402-3281; E-mail: pmeltzer@nhgri.nih.gov.

[3] The abbreviations used are: GIST, gastrointestinal stromal tumor; ICC, interstitial cells of Cajal; CML, chronic myeloid leukemia; IHC, immunohistochemistry; MDS, multidimensional scaling.

Materials and Methods

Tumor Samples and Cell Line. We obtained all tumor samples from the Cooperative Human Tissue Network. GIST samples (Table 1) were all malignant tumors with spindle cell morphology except for sample 11, which had mixed spindle/epithelioid morphology. DNA was extracted with a Qiagen Blood and Cell Culture DNA Kit (Qiagen, Valencia, CA). Total cellular RNA was isolated from frozen tumor specimens and the reference cell line OsA-CL (8) by extraction with TRIzol Reagent (Life Technologies, Inc., Gaithersburg, MD) and was further purified with the RNeasy kit (Qiagen). The osteosarcoma cell line OsA-CL was grown in RPMI 1640 containing FCS (10%), penicillin (50 units/ml), and streptomycin (50 μg/ml).

PCR Amplification and Sequencing Analysis. We used PCR to amplify genomic fragments of exons 9, 11, and 13 of the *KIT* gene for direct sequencing. Amplifications typically used 100 ng of genomic DNA in a 50-μl reaction, a hot start, and 35 cycles. Previously described primers were used with M13 tails: CK10.4F and CK11.4R for exon 11, CK9.1F and CK9.3R for exon 9, and CD13.1F and CD13.2R for exon 13 (9, 10). The PCR products were purified, by use of a Qiagen PCR purification kit (Qiagen) and the Qiagen BIOROBOT 9600 dual vacuum system. Sequencing reactions of the PCR products were set up in a 96-well format using the 3700 Big Dye Terminator Chemistry (PE/Applied Biosystems, Foster City, CA) and placed on an MJ Tetrad. The sequencing reactions were purified in a 96-well Sephadex G-50 plate (University of Oklahoma Advanced Center for Genome Technology, Norman, OK), dried, and dissolved/denatured in 10 μl of Hi-Di formamide loading buffer at 95°C for 3 min. The samples were run on a 3700 DNA Analyzer (PE/Applied Biosystems).

IHC. We performed IHC with a rabbit polyclonal anti-KIT (CD117) antibody (A-4502, 1:50 dilution; DAKO Corporation, Carpinteria, CA) on paraffin-embedded tissue sections, using the avidin-biotin-peroxidase complex method (ABC Kit; Vector Laboratories, Burlingame, CA). To increase specificity and sensitivity, we used microwave antigen retrieval and an overnight incubation at 4°C with KIT.

cDNA Microarrays and Image Analysis. The 13,826 human cDNAs used in this study were obtained under a Cooperative Research and Development Agreement with Research Genetics (Huntsville, AL). Gene names are according to build 138 of the Unigene human sequence collection.[4] PCR products generated from these clones were printed onto glass slides as described previously (11). Microarrays were hybridized and scanned, and image analysis was performed as described previously (12, 13). Briefly, fluorescently labeled cDNA was synthesized from ~90 μg of tumor RNA or ~45 μg of cell line RNA by oligo(dT)-primed polymerization in the presence of Cy3 or Cy5 dUTP, respectively (Amersham Pharmacia Biotech, Piscataway, NJ). The reference cell line was included in each hybridization to allow for normalization of each clone's expression relative to the reference for each sample. Image analyses were performed with DeArray software (13).[5] The two fluorescent images (red and green channels) obtained constituted the raw data from which differential gene expression ratio values were calculated. All data were entered into a database, using Filemaker Pro software.

Statistical Analyses. The hierarchical clustering analyses and the MDS plot were generated as described previously (14, 15). To filter the data set and select genes significantly expressed in GISTs, we required the average natural

[4] http://www.ncbi.nlm.nih.gov/UniGene/build.html.

[5] http://www.nhgri.nih.gov/DIR/microarray.

Table 1 *Study material*

Tumor	Diagnosis	Age (yrs)/Sex	Sample characteristics	Tumor size[a] (cm)	KIT IHC[b]
1	GIST	72/F	Intra-abdominal extension	16	+
2	GIST	60/M	Intra-abdominal extension	12.6	+
3	GIST	54/M	Intra-abdominal extension	17	+
4	GIST	72/F	Stomach primary	8.2	+
5	GIST	62/F	Intra-abdominal extension	16.8	+
6	GIST	71/M	Intra-abdominal extension	5	+
7	GIST	41/F	Intra-abdominal extension	45	+
8	GIST	84/M	Stomach primary	3	+
9	GIST	71/F	Rectal primary	7	+
10	GIST	41/M	Rectal primary	10	+
11	GIST	63/M	Stomach primary	9.5	+
12	GIST	50/M	Liver metastasis	1.5	+
13	GIST	60/F	Intra-abdominal extension	8.5	NA
14	Sarcomatoid mesothelioma	67/F	Lung	27.5	−
15	Spindle cell sarcoma	56/F	Lung	11	
16	Spindle cell sarcoma	58/F	Breast	24	−
17	Spindle cell sarcoma	73/M	Back	11	−
18	Spindle cell sarcoma	75/M	Thigh	3.7	−
19	Fibromatosis	38/M	Foot	14.4	−

[a] Maximum dimension.
[b] Immunohistochemical staining for KIT: +, strong staining; −, no staining; NA, not available.

logarithm (ln) of the relative red (tumor) intensity (16) for the mutation positive samples to exceed ln(1.5) for each clone. The genes were ranked according to the signal-to-noise ratio, and a weighted list of genes was generated as follows (17): Let $[\mu_+(g),\sigma_+(g)]$ and $[\mu_-(g),\sigma_-(g)]$ denote the means and SDs of the natural logarithm of the expression levels (calibrated ratios) of the gene g in the samples from mutation-positive GISTs and spindle cell tumors, respectively. The weight for each gene is defined as: $w(g, \pm) = |\mu_+(g) - \mu_-(g)|/[\sigma_+(g) + \sigma_-(g)]$. When $[\mu_+(g) - \mu_-(g)]$ is positive, the gene g is more highly expressed in the mutation-positive group, whereas when it is negative, the gene g is more highly expressed in the spindle cell group. A random permutation test was used to determine whether a gene was significantly associated with distinguishing the two classes. We randomly permuted the labels of the samples 100,000 times and for each gene calculated the probability α of obtaining a larger weight for a random permutation than for the separation of the two groups.

Results and Discussion

We identified 13 GISTs with mutations in the *KIT* gene by direct sequencing of exons 9, 11, and 13. Twelve cases had 3- to 42-bp deletions in exon 11, corresponding to amino acid residues Tyr^{553} to Asp^{579} of the juxtamembrane domain (Fig. 1). The final case had a mutation in exon 9 that was identical to the previously described 6-bp duplication encoding amino acid residues Ala^{502} and Tyr^{503} of the extracellular domain (18). KIT protein expression was confirmed by IHC with the anti-KIT (CD117) antibody (Fig. 2*B* and Table 1). For comparison, we selected a group of six tumors with spindle cell morphology located outside the digestive tract and negative for KIT protein expression (Fig. 2*A* and Table 1).

Cy3-labeled tumor cDNA was hybridized to 13,826-element cDNA microarrays relative to Cy5-labeled reference cDNA from the cell line OsA-CL. Expression profiles based on calculated intensity ratios were obtained for all 19 tumors presented in Table 1. The three-dimensional MDS plot based on overall gene expression from all analyzed cDNA clones indicated a distinct clustering of the GIST samples separate from the spindle cell tumors (Fig. 2*C*). The filter based on the average natural logarithm of relative red intensity (16) for the mutation-positive samples was set at $\geq$ln(1.5) to select for genes having a significant expression in GISTs. This requirement yielded a list of 1987 cDNAs (available on-line at the National Human Genome Research Institute web

```
WT       KPMYEVQWKVVEEINGNNYVYIDPTQLPYD
TUMOR
1        KPMYEVQ--VVEEINGNNYVYIDPTQLPYD
2        KPM----WKVVEEINGNNYVYIDPTQLPYD
3        KPMYE----VVEEINGNNYVYIDPTQLPYD
4        KPMYE----VVEEINGNNYVYIDPTQLPYD
5        KPMYEVQWK---EINGNNYVYIDPTQLPYD
6        KPMYEVQWKVVEEINGNNYVYIDPTQLPY-
7        KPMYEVQWKVVEET--------------YD
8        KPMYEVQWKV-EEINGNNYVYIDPTQLPYD
9        KPMYEVQW---EEINGNNYVYIDPTQLPYD
10       KPMYEVQ--VVEEINGNNYVYIDPTQLPYD
11       KPMYEVQC--VEEINGNNYVYIDPTQLPYD
12       KPMYEVQWKVVEEINGNN-------QLPYD
```

Fig. 1. Exon 11 *KIT* mutations in 12 GIST samples. The wild-type (*WT*) sequence of the amino acids encoded by exon 11 is shown at the *top*. The mutated sequences are listed according to the tumor number, indicated at the *left*.

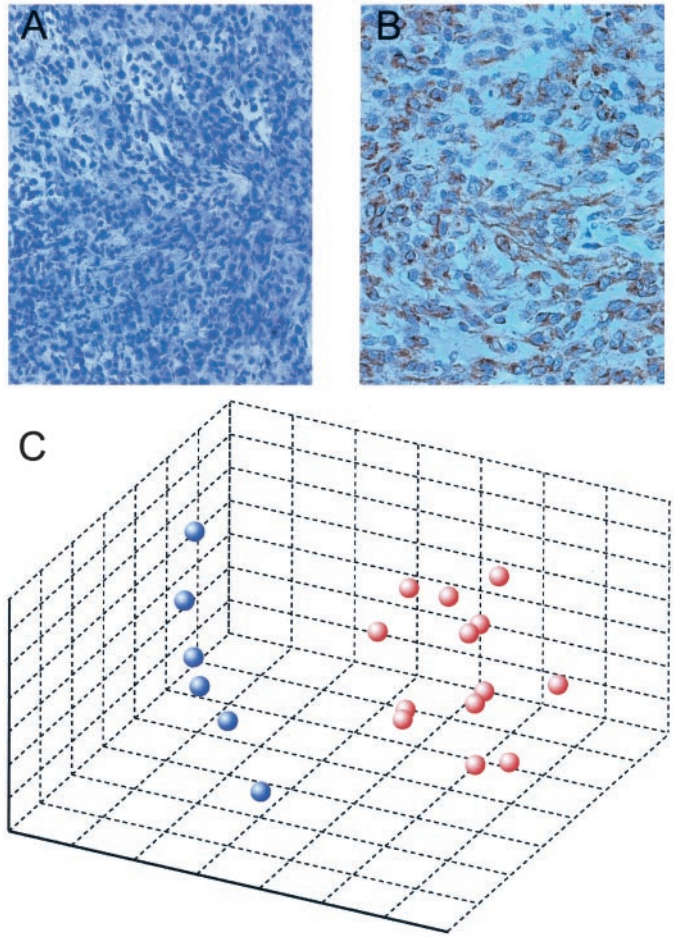

Fig. 2. IHC using anti-KIT antibody. All of the spindle cell sarcomas were negative for *KIT* expression, as demonstrated in tumor sample 17 (*A*; magnification, ×200), whereas all *KIT* mutation-positive tumors showed KIT immunoreactivity as demonstrated in tumor sample 7 (*B*; magnification, ×400). *C*, MDS plot based on the overall gene expression for all 19 tumor samples. The similarity of gene expression profiles between any pair of tumor samples was assessed by Pearson correlation coefficients based on expression levels from all genes with good measurement quality. The MDS plot, in which *orange dots* represent mutation-positive GISTs and *blue dots* represent spindle cell sarcomas, depicts the location of each sample in a viewable three-dimensional space. Samples with similar gene expression profiles are near each other, separate from other dissimilar groups.

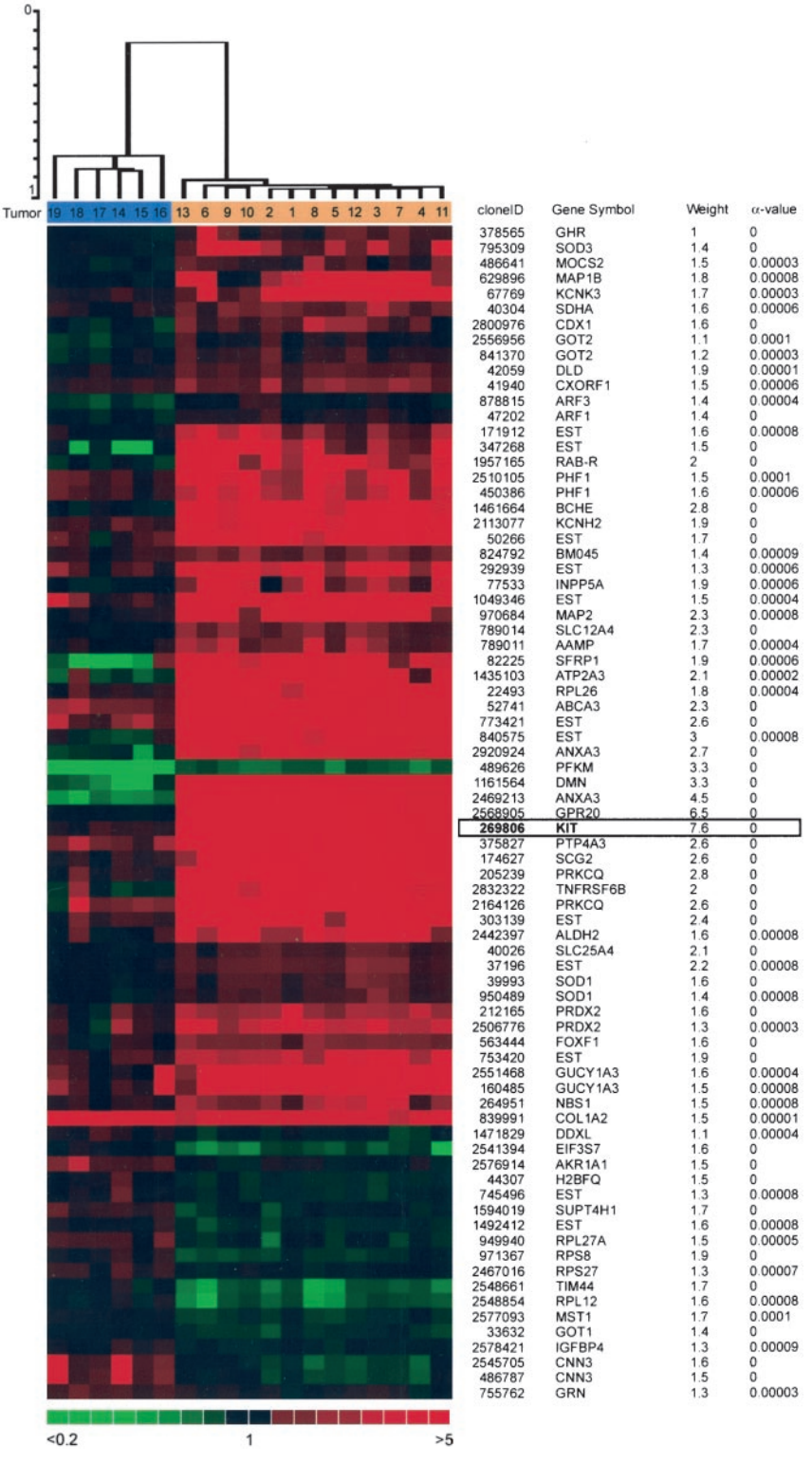

cloneID	Gene Symbol	Weight	α-value
378565	GHR	1	0
795309	SOD3	1.4	0
486641	MOCS2	1.5	0.00003
629896	MAP1B	1.8	0.00008
67769	KCNK3	1.7	0.00003
40304	SDHA	1.6	0.00006
2800976	CDX1	1.6	0
2556956	GOT2	1.1	0.0001
841370	GOT2	1.2	0.00003
42059	DLD	1.9	0.00001
41940	CXORF1	1.5	0.00006
878815	ARF3	1.4	0.00004
47202	ARF1	1.4	0
171912	EST	1.6	0.00008
347268	EST	1.5	0
1957165	RAB-R	2	0
2510105	PHF1	1.5	0.0001
450386	PHF1	1.6	0.00006
1461664	BCHE	2.8	0
2113077	KCNH2	1.9	0
50266	EST	1.7	0
824792	BM045	1.4	0.00009
292939	EST	1.3	0.00006
77533	INPP5A	1.9	0.00006
1049346	EST	1.5	0.00004
970684	MAP2	2.3	0.00008
789014	SLC12A4	2.3	0
789011	AAMP	1.7	0.00004
82225	SFRP1	1.9	0.00006
1435103	ATP2A3	2.1	0.00002
22493	RPL26	1.8	0.00004
52741	ABCA3	2.3	0
773421	EST	2.6	0
840575	EST	3	0.00008
2920924	ANXA3	2.7	0
489626	PFKM	3.3	0
1161564	DMN	3.3	0
2469213	ANXA3	4.5	0
2568905	GPR20	6.5	0
269806	**KIT**	7.6	0
375827	PTP4A3	2.6	0
174627	SCG2	2.6	0
205239	PRKCQ	2.8	0
2832322	TNFRSF6B	2	0
2164126	PRKCQ	2.6	0
303139	EST	2.4	0
2442397	ALDH2	1.6	0.00008
40026	SLC25A4	2.1	0
37196	EST	2.2	0.00008
39993	SOD1	1.6	0
950489	SOD1	1.4	0.00008
212165	PRDX2	1.6	0
2506776	PRDX2	1.3	0.00003
563444	FOXF1	1.6	0
753420	EST	1.9	0
2551468	GUCY1A3	1.6	0.00004
160485	GUCY1A3	1.5	0.00008
264951	NBS1	1.5	0.00008
839991	COL1A2	1.5	0.00001
1471829	DDXL	1.1	0.00004
2541394	EIF3S7	1.6	0
2576914	AKR1A1	1.5	0
44307	H2BFQ	1.5	0
745496	EST	1.3	0.00008
1594019	SUPT4H1	1.7	0
1492412	EST	1.6	0.00008
949940	RPL27A	1.5	0.00005
971367	RPS8	1.9	0
2467016	RPS27	1.3	0.00007
2548661	TIM44	1.7	0
2548854	RPL12	1.6	0.00008
2577093	MST1	1.7	0.0001
33632	GOT1	1.4	0
2578421	IGFBP4	1.3	0.00009
2545705	CNN3	1.6	0
486787	CNN3	1.5	0
755762	GRN	1.3	0.00003

Fig. 3. Hierarchical clustering dendrogram and gene expression data from GISTs and spindle cell tumors. The dendrogram (shown at the *top*) was generated with the subset of 113 cDNAs with $\alpha \leq 0.0001$ for separation of GISTs and spindle cell tumors. The *ruler* shows the Pearson correlation between samples. These 113 elements represent 77 unique cDNA clones from 69 genes. Gene expression data from the 77 unique cDNA clones are displayed. The hierarchical clustering presents the clustered samples in *columns* and the clustered genes in *rows*. A pseudo-colored representation of gene expression ratios is shown according to the scale at the *bottom*.

site[5]). These genes were ranked to generate a weighted gene list (17), and a random permutation test was used to determine how many top-ranked genes significantly distinguished the two classes. We used α, the probability of a larger weight for a random permutation than for separation of GISTs *versus* spindle cell tumors, to assess the most significant discriminatory genes. We found 113 cDNAs with $\alpha \leq 0.0001$. These 113 clones represented 77 unique cDNA sequences from 69 different genes (Fig. 3).

The most highly ranked gene on the discriminator list was *KIT* itself, which was highly expressed in every GIST studied (Fig. 3), and it might be expected that other genes related to *KIT* function will also be highly expressed. Similarly, given the pacemaker activity of the ICC, one would expect a tumor arising from these cells to express genes related to their electrophysiological function, *i.e.*, ion channels, receptors, and signal transduction molecules. For example, we found that the genes encoding the signaling molecules

G-protein-coupled receptor 20 (*GPR20*) and protein kinase C θ (*PRKCQ*) were highly expressed in GISTs and clustered tightly with *KIT*. Both G-protein-coupled receptors and protein kinase C are suggested as mediators of tyrosine kinase function (19), which suggests a possible relationship of *PRKCQ* and *GPR20* to the *KIT* pathway. Genes encoding ion channels that were highly expressed in GISTs included the potassium channel genes *KCNK3* and *KCNH2*. We also detected expression of the gene encoding secretogranin II (*SCG2*), the precursor of the neuropeptide secretoneurin, which is suggested to have a role in modulation of gastrointestinal motility (20). We believe that these observations together support the hypothesis that GISTs originate from a stem cell with the ability to differentiate toward an ICC phenotype (3, 4). We also found uniform and high expression of the gene encoding tumor necrosis factor receptor subfamily 6b (*TNFRSF6B*), also known as DcR3 or M68, which recently was shown to be overexpressed in gastrointestinal adenocarcinomas (21).

Traditional immunohistochemical staining patterns of GISTs show CD34 positivity in ~70% of the tumors, which helps narrow the differential diagnosis of GIST from other mesenchymal tumors (1, 3). Our cDNA array data showed high expression of *CD34* mRNA in 9 of our 13 studied tumors (data not shown), a proportion in total agreement with previous observations. The *CD34* gene was the 376th discriminator on our weighted list (weight, 0.9; $\alpha \sim 0.008$).[5]

One striking observation is the remarkable consistency of the gene expression pattern within the GIST group. When we applied hierarchical clustering (14, 15) based on the 1987 cDNAs as described above, all GIST samples were placed into one branch, with a Pearson correlation >0.84. The Pearson correlation increased to >0.91, as illustrated by the dendrogram in Fig. 3, when we applied a hierarchical clustering analysis using the subset of 113 cDNAs with $\alpha \leq 0.0001$. The extremely high correlation between different tumor samples contrasts with that observed in the more common epithelial cancers (22–24). This observation is consistent with a model for the pathogenesis of GIST based on the expansion of an ICC clone with an activating mutation in *KIT* (4), but without the extreme genetic instability commonly seen in epithelial cancers.

A recent report showed a remarkable effect of the tyrosine kinase inhibitor STI571 in a patient with GIST and multiple intra-abdominal, mesenteric, and liver tumors (7). This drug was recently approved for the treatment of CML, where it acts through inhibition of the BCR-ABL tyrosine kinase characteristic of CML (5, 6). GIST is defined by its KIT protein overexpression, which frequently is accompanied by activating mutations (1). The reported effectiveness of STI571 also in a case with advanced (mutation-positive) GIST (7) suggests that the uncontrolled cell growth in GIST is primarily driven by its KIT overexpression. Like chronic phase CML, GIST may represent clonal expansion of a progenitor cell that has acquired an activating kinase mutation and relatively few additional genetic changes. The great similarity in gene expression pattern among our GIST samples is consistent with this concept. Previous reports have shown that GISTs frequently can acquire specific secondary genetic changes, especially loss of chromosomes 14q and 22q (25–27). The effects of these changes on gene expression and clinical behavior have not been fully elucidated, and further studies are needed to address these questions. Because our sample set primarily included large tumors with an aggressive clinical behavior, it is possible that very small tumors or benign GISTs differ in their gene expression patterns. Nonetheless, our data suggest that mutation-positive GISTs display a uniform expression profile consistent with a relatively simple pattern of genetic alterations. These observations lead us to believe that STI571 may be active in a high proportion of *KIT* mutation-positive GISTs. Our gene expression data are also consistent with the clinical behavior of GIST, which is almost invariably confined to the abdomen without distant metastases (1), and may bode well for a high rate of response to STI571.

Acknowledgments

We thank Kimberly A. Gayton, Darryl Leja, John Leuders, Tracy Y. Moses, Christiane M. Robbins, and Robert L. Walker for excellent technical assistance. Tumor samples were obtained from the Cooperative Human Tissue Network, which is funded by the National Cancer Institute.

References

1. Miettinen, M., and Lasota, J. Gastrointestinal stromal tumors—definition, clinical, histological, immunohistochemical, and molecular genetic features and differential diagnosis. Virchows Arch., *438:* 1–12, 2001.
2. Strickland, L., Letson, G. D., and Muro-Cacho, C. A. Gastrointestinal stromal tumors. Cancer Control, *8:* 252–261, 2001.
3. Kindblom, L. G., Remotti, H. E., Aldenborg, F., Meis-Kindblom, J. M. Gastrointestinal pacemaker cell tumor (GIPACT): gastrointestinal stromal tumors show phenotypic characteristics of the interstitial cells of Cajal. Am. J. Pathol., *152:* 1259–1269, 1998.
4. Hirota, S., Isozaki, K., Moriyama, Y., Hashimoto, K., Nishida, T., Ishiguro, S., Kawano, K., Hanada, M., Kurata, A., Takeda, M., Tunio, G. M., Matsuzawa, Y., Kanakura, Y., Shinomura, Y., and Kitamura, Y. Gain-of-function mutations of c-kit in human gastrointestinal stromal tumors. Science (Wash. DC), *279:* 577–580, 1998.
5. Druker, B. J., Tamura, S., Buchdunger, E., Ohno, S., Segal, G. M., Fanning, S., Zimmermann, J., and Lydon N. B. Effects of a selective inhibitor of the Abl tyrosine kinase on the growth of Bcr-Abl positive cells. Nat. Med., *2:* 561–566, 1996.
6. Druker, B. J., Talpaz M., Resta, D. J., Peng, B., Buchdunger, E., Ford, J. M., Lydon N. B., Kantarjian H., Capdeville, R., Ohno-Jones, S., and Sawyers, C. L. Efficacy and safety of a specific inhibitor of the Bcr-Abl tyrosine kinase in chronic myeloid leukemia. N. Engl. J. Med., *344:* 1031–1037, 2001.
7. Joensuu, H., Roberts, P. J., Sarlomo-Rikala, M., Andersson, L. C., Tervahartiala, P., Tuveson, D., Silberman, S. L., Capdeville, R., Dimitrijevic, S., Druker, B., and Demetri, G. D. Effect of the tyrosine kinase inhibitor STI571 in a patient with a metastatic gastrointestinal stromal tumor. N. Engl. J. Med., *344:* 1052–1056, 2001.
8. Roberts, W. M., Douglass, E. C., Peiper, S. C., Houghton, P. J., and Look, A. T. Amplification of the *gli* gene in childhood sarcomas. Cancer Res., *49:* 5407–5413, 1989.
9. Lasota, J., Wozniak, A., Sarlomo-Rikala, M., Rys, J., Kordek, R., Nassar, A., Sobin, L. H., and Miettinen M. Mutations in exons 9 and 13 of the KIT gene are rare events in gastrointestinal stromal tumors. Am. J. Pathol., *157:* 1091–1095, 2000.
10. Miettinen, M., Sarlomo-Rikala, M., Sobin, L. H., and Lasota J. Gastrointestinal stromal tumors and leiomyosarcomas in the colon. Am. J. Surg. Pathol., *24:* 1339–1352, 2000.
11. DeRisi, J., Penland, L., Brown, P. O., Bittner, M. L., Meltzer, P. S., Ray, M., Chen, Y., Su, Y. A., and Trent, J. M. Use of a cDNA microarray to analyse gene expression patterns in human cancer. Nat. Genet., *14:* 457–460, 1996.
12. Khan, J., Simon, R., Bittner, M., Chen, Y., Leighton, S. B., Pohida, T., Smith, P. D., Jiang, Y., Gooden, C., Trent, J. M., and Meltzer P. S. Gene expression profiling of alveolar rhabdomyosarcoma with cDNA microarrays. Cancer Res., *58:* 5009–5013, 1998.
13. Chen, Y., Dougherty, E. R., and Bittner, M. L. Ratio-based decisions and the quantitative analysis of cDNA microarray images. Biomed. Opt., *2:* 364–374, 1997.
14. Bittner, M., Meltzer, P., and Trent, J. Data analysis and integration: of steps and arrows. Nat. Genet., *22:* 213–215, 1999.
15. Bittner, M., Meltzer, P., Chen, Y., Jiang, Y., Seftor, E., Hendrix, M., Radmacher, M., Simon, R., Yakhini, Z., Ben-Dor, A., Sampas, N., Dougherty, E., Wang, E., Marincola, F., Gooden, C., Leuders, J., Glatfelter, A., Pollock, P., Carpten, J., Gillanders, E., Leja, D., Dietrich, K., Beaudry, C., Berens, M., Alberts, D., Sondak, V., Hayward, N., and Trent, J. Molecular classification of cutaneous malignant melanoma by gene expression profiling. Nature (Lond.), *406:* 536–540, 2000.
16. Khan, J., Wei, J. S., Ringnér, M., Saal, L. H., Ladanyi, M., Westermann, F., Schwab, M., Antonescu, C., Peterson, C., and Meltzer, P. S. Classification and diagnostic prediction of cancers using gene expression profiling and artificial neural networks. Nat. Med., *7:* 673–678, 2001.
17. Golub, T. R., Slonim, D. K., Tamayo, P., Huard, C., Gaasenbeek, M., Mesirov, J. P., Coller, H., Loh, M. L., Downing, J. R., Caligiuri, M. A., Bloomfield, C. D., and Lander, E. S. Molecular classification of cancer: class discovery and class prediction by gene expression monitoring. Science (Wash. DC), *286:* 531–537, 1999.
18. Lux, M. L., Rubin, B. P., Biase, T. L., Chen, C-J., Maclure, T., Demetri, G., Xiao, S., Singer S., Fletcher, C. D. M., and Fletcher J. A. KIT extracellular and kinase domain mutations in gastrointestinal stromal tumors. Am. J. Pathol., *156:* 791–795, 2000.
19. Luttrell, L. M., Daaka, Y., and Lefkowitz, J. Regulation of tyrosine kinase cascades by G-protein coupled receptors. Curr. Opin. Cell Biol., *11:* 177–183, 1999.
20. Wiedermann, C. J. Secretoneurin: a functional neuropeptide in health and disease. Peptides., *21:* 1289–1298, 2000.
21. Bai, C., Connolly, B., Metzker, M. L., Hilliard, C. A., Liu, X., Sandig, V., Soderman, A., Galloway, S. M., Liu, Q., Austin, C. P., and Caskey, C. T. Overexpression of M68/DcR3 in a human gastrointestinal tract tumors independent of gene amplification

and its location in a four-gene cluster. Proc. Natl. Acad. Sci. USA, *97:* 1230–1235, 2000.

22. Perou, C. M., Sørlie, T., Eisen, M. B., van de Rijn, M., Jeffrey, S. S., Rees, C. A., Pollack, J. R., Ross, D. T., Johnsen, H., Akslen, L. A., Fluge, Ø., Pergamenschikov, A., Williams, C., Zhu, S. X., Lønning, P. E., Børresen-Dale, A-L., Brown, P. O., and Botstein, D. Molecular portraits of human breast tumours. Nature (Lond.), *406:* 747–752, 2000.
23. Scherf, U., Ross, D. T., Waltham, M., Smith, L. H., Lee, J. K., Tanabe, L., Kohn, K. W., Reinhold, W. C., Myers, T. G., Andrews, D. T., Scudiero, D. A., Eisen, M. B., Sausville, E. A., Pommier, Y., Botstein, D., Brown, P. O., and Weinstein, J. N. A gene expression database for the molecular pharmacology of cancer. Nat. Genet., *24:* 236–244, 2000.
24. Notterman, D. A., Alon, U., Sierk, A. J., and Levine, A. J. Transcriptional gene expression profiles of colorectal adenoma, adenocarcinoma, and normal tissue examined by oligonucleotide arrays. Cancer Res., *61:* 3124–3130, 2001.
25. Breiner, J. A., Meis-Kindblom, J., Kindblom, L-G., McComb, E., Liu, J., Nelson, M., and Bridge J. A. Loss of 14q and 22q in gastrointestinal stromal tumors (pacemaker cell tumors). Cancer Genet. Cytogenet., *120:* 111–116, 2000.
26. El-Rifai, W., Sarlomo-Rikala, M., Andersson, L. C., Knuutila, S., Miettinen, M. DNA sequence copy number changes in gastrointestinal stromal tumors: tumor progression and prognostic significance. Cancer Res., *60:* 3899–3903, 2000.
27. Debiec-Rychter, M., Lasota, J., Sarlomo-Rikala, M., Kordek, R., and Miettinen, M. Chromosomal aberrations in malignant gastrointestinal stromal tumors: correlation with c-KIT gene mutation. Cancer Genet. Cytogenet., *128:* 24–30, 2001.